Supporting Information

Microporous Metal-Organic Framework Based on Ligand-Truncation Strategy with High Performance for Gas Adsorption and Separation

Jianqiang Liu,[‡a] *Wenjing Wang,*[‡bc] *Zhidong Luo,*[a] *Baohong Li,*[a] *and Daqiang Yuan*[b*]

[a]School of Pharmacy, Guangdong Medical University, Dongguan, 523808, China.

[b]State Key Laboratory of Structural Chemistry, Fujian Institute of Research on the Structure of Matter, Chinese Academy of Sciences, Fuzhou, 350002, China.

[c]University of the Chinese Academy of Sciences, Beijing, 100049, China.

Supplementary Figures

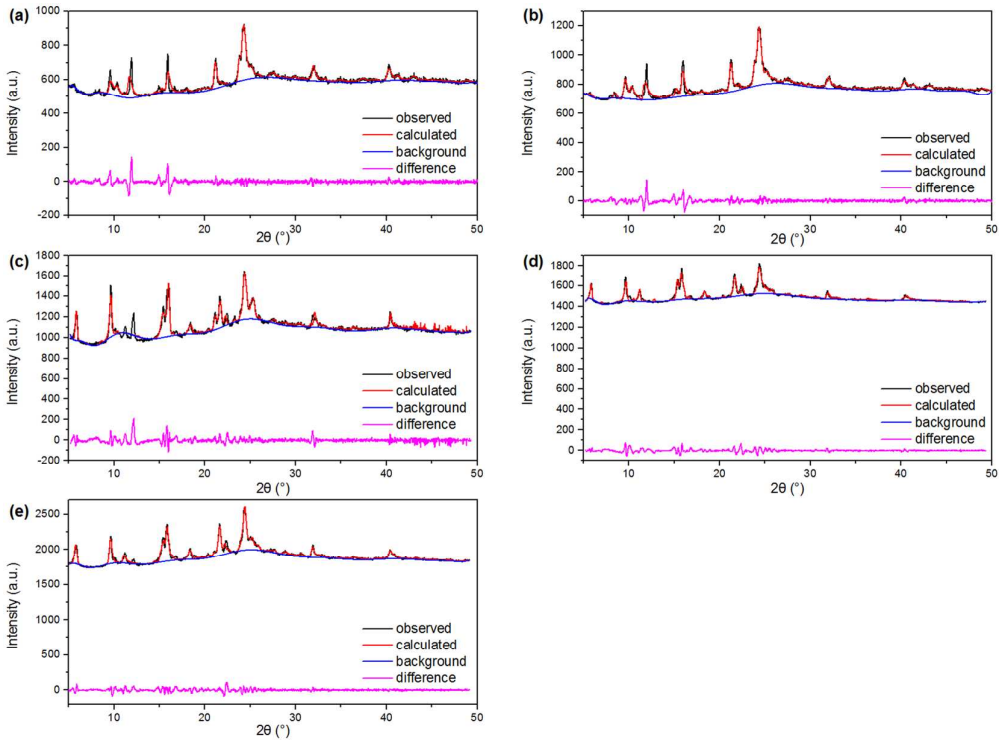

Figure S1. LeBail method fit to PXRD data for the samples of **1**. (a) as-synthesized, (b) activated, (c) after gas desorption, (d) immersed in CH_2C1_2 (e) immersed in CH_3OH.

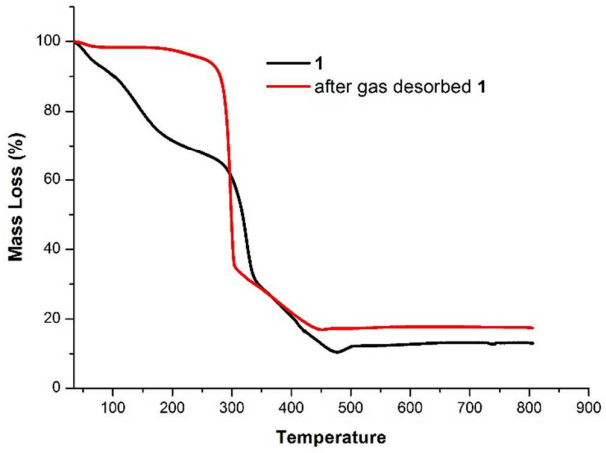

Figure S2. View of the TGA for as-synthesized and gas desorbed samples in **1**.

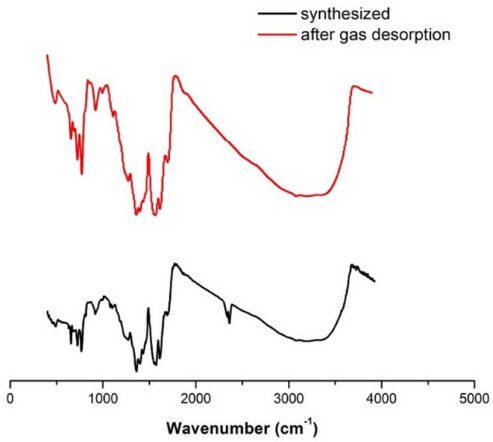

Figure S3. View of the IR for as-synthesized and gas desorbed samples in **1**.

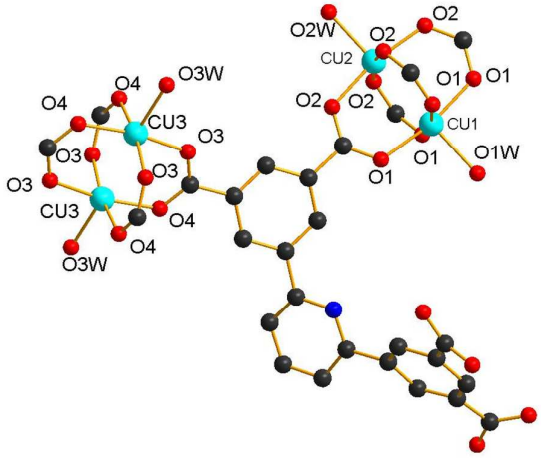

Figure S4. View of coordination environment of metal ions and ligands in **1**.

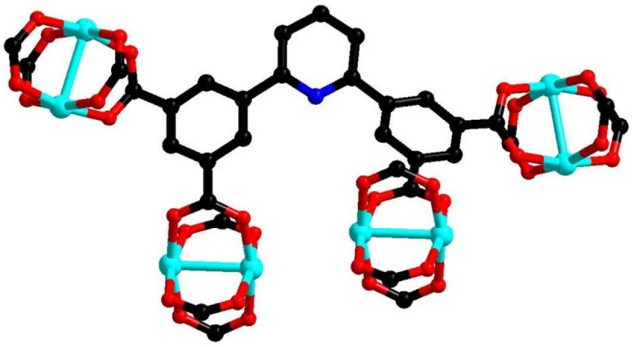

Figure S5. The L^{4-} ligands can be regarded as 4-c node linked by Cu_2 paddlewheel units

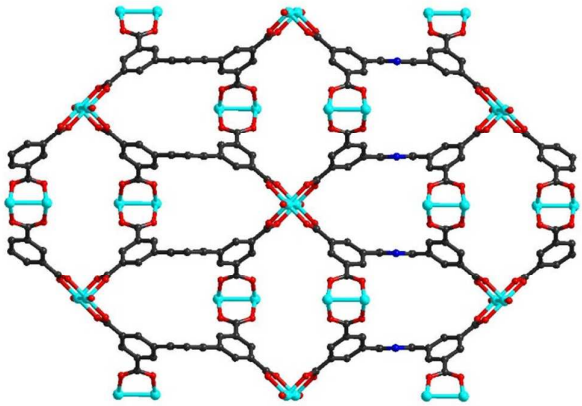

Figure S6. Two linked cages in the 3D network of **1**.

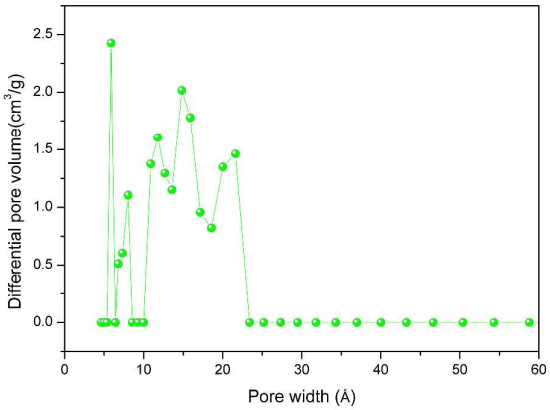

Figure S7. Pore size distributions analyzed by NLDFT methods.

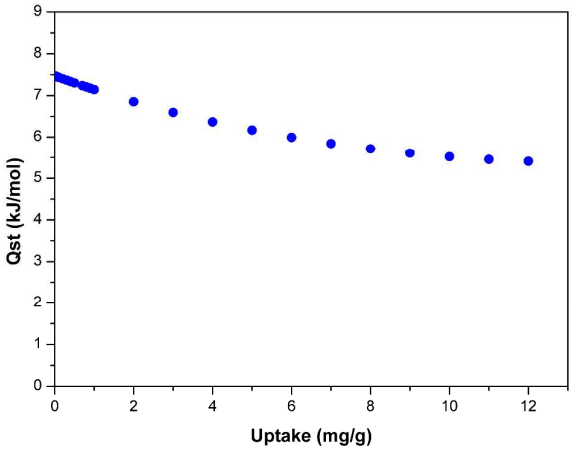

Figure S8. The Q_{st} of hydrogen for **1**

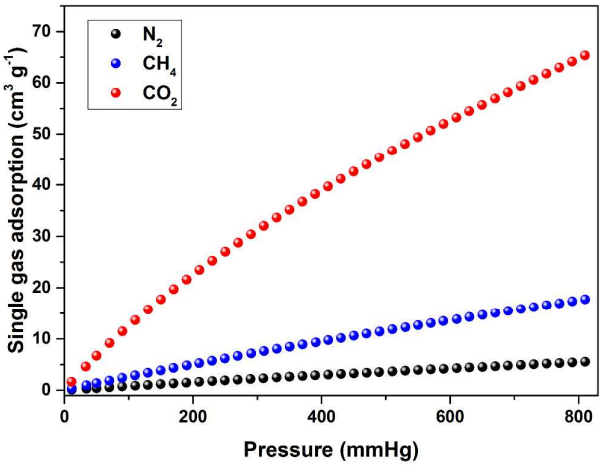

Figure S9. The single gas adsorption at 293 K

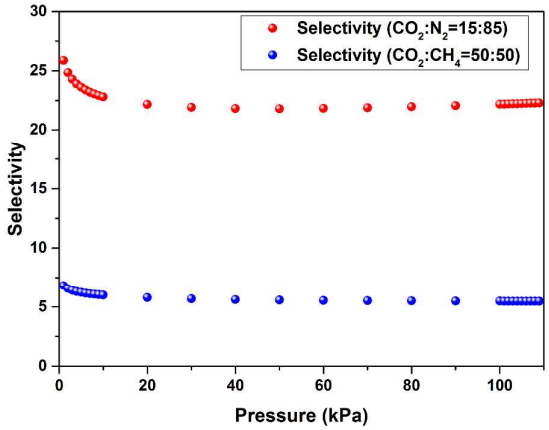

Figure S10. Adsorption selectivity of CO_2 over CH_4 or N_2 at 293 K

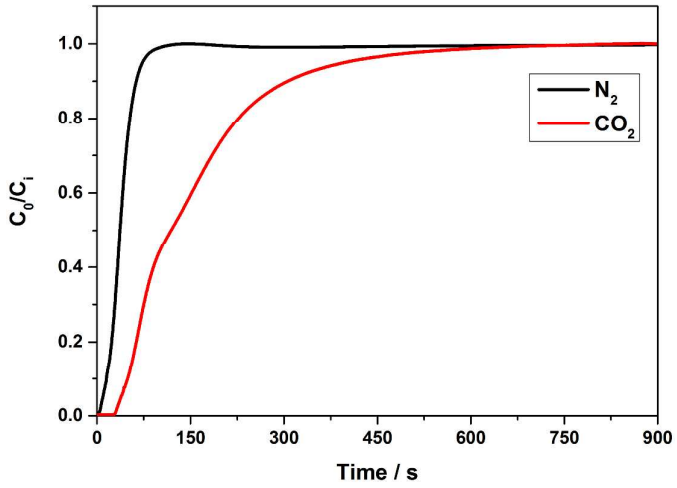

Figure S11. Breakthrough curves of **1** at 293 K and 1 bar

Table S1. Crystal data and structure refinement information for compound **1**

Crystal system	Cubic
Space group	orthorhombic
a, Å	13.8346(8)
b, Å	20.5675(11)
c, Å	30.1981(16)
V, Å ^{3}	8592.7(8)
Z	8
D_{calcd}, g/cm^3	1.100
μ, mm^{-1}	1.340
F(000)	3616
θ Range, deg	2.2287- 25.5585
Reflection collected	14531
Independent reflections (R_{int})	0.0918
Reflections with $I > 2\sigma(I)$	4072
R_1, wR_2 ($I > 2\sigma(I)$)*	0.0528, 0.1474
R_1, wR_2 (all data)**	0.0854, 0.1615

* $R = \sum(F_o - F_c)/\sum(F_o)$, ** $wR_2 = \{\sum[w(F_o^2 - F_c^2)^2]/\sum(F_o^2)^2\}^{1/2}$.

Table S2. Selected bond distances (Å) and angles (º) of structure **1**

Cu1-O1$^{\#1}$	1.968(3)	Cu1-O1w$^{\#2}$	2.139(6)
Cu1-Cu2	2.6672(14)	Cu2-O2$^{\#3}$	1.973(3)
Cu2-O2w	2.096(6)	Cu3-O4	1.956(3)
Cu3-O3$^{\#4}$	1.976(3)	Cu3-Cu3	2.6559(16)
O1-Cu1-O1	91.0(2)	O1-Cu1-O1w	95.53(9)
O2-Cu2-O2	90.3(2)	O2-Cu2-O2w	96.13(9)
O2w-Cu2-Cu1	180	O4-Cu3-O4	87.57(19)
O4-Cu3-O3	168.26(15)	O3-Cu3-O3	90.21(19)
O4-Cu3-O3w	97.13(16)	O3-Cu3-O3w	94.56(15)

#1: -x, -y+1/2, z; #2: -x, y+1/2, -z; #3: x, -y, -z; #4: x+1/2, y+1/2, z+1/2

Table S3. The pattern matching analysis data for **1** by the LeBail route

	As-synthesized	Dehydrated	After gas adsorption	Immersed in CH_2Cl_2	Immersed in CH_3OH
a (Å)	13.9158	13.8691	13.8376	13.7962	13.8631
b (Å)	20.7448	20.7278	20.6047	20.2590	20.6908
c (Å)	30.2311	30.2448	30.1585	30.0488	30.4623
α (°)	90	90	90	90	90
β (°)	90	90	90	90	90
γ (°)	90	90	90	90	90
V ($Å^3$)	8727.10	8694.68	8598.78	8398.59	8737.78
R_p	1.338	0.999	1.349	0.510	0.621
R_{wp}	2.389	1.655	2.133	0.816	0.935
R_{exp}	4.098	3.556	2.996	2.576	2.274
χ^2	0.340	0.217	0.507	0.100	0.169